

Numerical Simulation of Two-Phase Water-Oil Flow in a Horizontal Pipe Using the Smoothed Particle Hydrodynamics Method[☆]

Simulação Numérica do Escoamento Bifásico Óleo-Água em um Duto Horizontal Empregando o Método Smoothed Particle Hydrodynamics

Naim Jessé dos Santos Carvalho[†], Grazione de Souza, Helio Pedro Amaral Souto

Polytechnic Institute, Rio de Janeiro State University, Nova Friburgo, Brazil

[†]**Corresponding author:** njscarvalho@iprj.uerj.br

Abstract

In this work, the numerical code DualPhysics, based on the Lagrangian particle and mesh free method Smoothed Particle Hydrodynamics, has been employed to solve the slightly compressible isothermal two-phase water-oil flow. The continuity and momentum equations were solved, and we used the modified Tait equation of state to determine the pressure. To validate the numerical code, we solved the modified Couette flow of two fluids. As a practical case, we solved the isothermal and two-dimensional two-phase water-oil flow. The mixing of the fluids occurs after passing through a 45 degree Y junction placed at the entrance of the horizontal pipeline. Results showed the potential for using the numerical code, although some modifications and alterations are still necessary to solve practical problems.

Keywords

Computational Fluid Dynamics • Two-Phase Flows • Smoothed Particle Hydrodynamics

Resumo

O código numérico DualPhysics, baseado no método de partículas lagrangiano e livre de malha Smoothed Particle Hydrodynamics, foi empregado na resolução do escoamento bifásico óleo-água isotérmico e ligeiramente compressível. São resolvidas as equações da continuidade, do momentum e a equação de estado de Tait modificada é empregada na determinação da pressão. Na validação do código numérico, considerou-se o escoamento de Couette de dois fluidos com massa específica e viscosidade diferentes. Como exemplo de aplicação, resolveu-se numericamente o escoamento bifásico água-óleo isotérmico e bidimensional, onde os fluidos são misturados através de uma junção em Y de 45 graus colocada na entrada do duto horizontal. Os resultados mostraram o potencial de uso do código numérico, embora ainda algumas modificações e alterações sejam necessárias para que ele possa ser utilizado na resolução de problemas práticos da engenharia de óleo e gás.

Palavras-chave

Fluidodinâmica Computacional • Escoamentos Bifásicos • Smoothed Particle Hydrodynamics

1 Introduction

Usually, the numerical solution of fluid flow problems is complex and requires efficient numerical methods, since we must simultaneously consider the continuity and the Navier-Stokes equations and, for non-isothermal flows,

[☆]This article is an extended version of the work presented at the Joint XXIV ENMC National Meeting on Computational Modelling and XII ECTM Meeting on Science and Technology of Materials, held in webinar mode, from October 13th to 15th, 2021.

the energy equation. Among the possibilities, it is worth highlighting the Smoothed Particle Hydrodynamics (SPH) method [1]. In such a method, we represent the domain using dynamic particles. Therefore, it does not require computational meshes.

In the SPH method, we can simulate phenomena of different scales, enabling the study of multiphase flows, high viscosity fluids, solid-fluid interfaces, and allowing several physical effects couplings. The literature provides a list of cases [2, 3] that can be treated by this method, starting from its initial proposition to simulate astrophysical problems, going through flows with high deformation rates, and even semi-incompressible and incompressible problems [1]. In this method, we discretize the domain using a set of particles, and we can assign to each particle mass, position, velocity, pressure, temperature, among others. These particles interact with others, obeying the governing equations, and they move in space as time progresses.

We can find two-phase flows in many fields: in chemical processes, in thermal systems with evaporators, in condensers and reactors, among others [4]. In the oil industry, they occur in production and transport along vertical and horizontal pipelines. In this situation, the operation conditions and geometry can lead to different shapes for the fluid interface, and we classify the flows according to the resulting patterns.

Knowing the flow pattern allows us, for example, to predict the operational parameters. Thus, it is possible to define flow characteristics that would minimize corrosion or erosion, allowing the optimization of the operating conditions [5].

We can find few studies using the SPH method to identify flow patterns in two-phase flows in pipelines. Douillet-Grellier et al. [6] identified the patterns considering two immiscible fluids and two geometric setups (horizontal and inclined pipes) for a set of velocity profiles. However, this was only possible after the introduction of several changes in the traditional SPH method formulation. For example, they modified the way we determine the density and the time step. Also, the authors introduced a repulsive force acting on the particles of the two phases, which are close to the separation interface, and an interaction force in the momentum equation to model the surface tension effects.

Alternatively, Alvarado-Rodríguez et al. [7] studied the two-phase flow with the SPH method and used an artificial viscosity and a particle shifting algorithm to maintain uniform particles distribution in the domain and thus prevent the appearance of regions that do not contain particles. The results were validated considering the Poiseuille and Couette two-phase flows. Furthermore, the authors also sought to determine the flow regimes observed in a horizontal pipeline. To this end, they considered the insertion of two flowing phases with different physical properties and applied four velocity profiles.

In this work, we obtain the results using the DualSPHysics software to simulate two-phase flows in pipelines, and we verify its feasibility for practical use.

2 Mathematical Model

We know that we must use a set of partial differential equations (PDEs) to describe an isothermal flow of compressible Newtonian fluids. We present here the governing equations using the Lagrangian description.

2.1 Continuity Equation

The continuity equation is obtained from the mass conservation and expresses the fact that in a given region of space without sources or sinks, the mass flow variation that enters and leaves such volume must be equal to the rate of change in the fluid density in a given time interval [8],

$$\frac{D\rho}{Dt} + \rho \nabla \cdot \mathbf{v} = 0 \quad (1)$$

where $D\rho/Dt$ denotes the material derivative, ρ is the density, whereas t is the time and \mathbf{v} is the velocity vector.

2.2 Momentum equation

We obtain this equation, which expresses the linear momentum conservation, considering the momentum balance. We deduce it from Euler's first law, which states that the variation rate of linear momentum must be equal to the sum of the forces acting on the body [8]:

$$\rho \frac{D\mathbf{v}}{Dt} = \nabla \cdot \mathbf{T} + \mathbf{f}_e \quad (2)$$

where \mathbf{T} is the stress tensor and \mathbf{f}_e represents the external forces acting on the fluid, usually due to the gravity.

The constitutive equation for the stress tensor, considering a compressible Newtonian fluid, is [8]

$$\mathbf{T} = -P\mathbf{I} + (\lambda \nabla \cdot \mathbf{v})\mathbf{I} + 2\mu\mathbf{D} \quad (3)$$

where P is the dynamic pressure, $\lambda = -\frac{2}{3}\mu$ (assuming the Stokes hypothesis), μ is the kinematic viscosity of the fluid, and \mathbf{D} is the symmetric part of the velocity gradient tensor.

Thus, the momentum equation can be rewritten as

$$\rho \frac{D\mathbf{v}}{Dt} = -\nabla P + \mu \nabla^2 \mathbf{v} - \frac{2}{3} \nabla (\mu \nabla \cdot \mathbf{v}) + \mathbf{f}_e \quad (4)$$

in which ∇P is the pressure force per unit volume, and $\mu \nabla^2 \mathbf{v}$ is the viscosity force per unit volume.

2.3 Equation of State for Pressure

In the SPH method, it is usual to consider incompressible fluids as quasi-compressible [9]. In this case, we adopt an equation of state to calculate the pressure as a function of density. For two-phase flows, the DualSPHysics code provides the model proposed by Mocos [10], which is a modified version of Tait's equation of state

$$P(\rho) = \frac{c_s^2 \rho_0}{\gamma} \left[\left(\frac{\rho}{\rho_0} \right)^\gamma - 1 \right] + P_f - a \rho^2 \quad (5)$$

where γ is the adiabatic expansion coefficient (usually $\gamma = 7$ [1]), ρ_0 is the reference density, c_s is the sound speed, and P_f is the background pressure. The last term represents the effects of cohesive forces acting on the particles for a given phase. The coefficient a is defined based on the properties of the different phases and the characteristic length of the problem, L :

$$a = 1.5g \left(\frac{\rho_w}{\rho_a} \right) L \quad (6)$$

where ρ_w and ρ_a are the reference density for each phase. The characteristic length is an empirical constant. It is related to the domain dimensions and the initial distance between particles. Douillet-Grellier et al. [6] suggest taking the pipe diameter as the characteristic length.

3 The Smoothed Particle Hydrodynamics method

During the code implementation and numerical solution using the SPH method, several steps and concepts are applied. A set of particles represent the domain at the beginning of the process. It is not required a connection between them. This characteristic defines the mesh-free nature of the method, which consists of the following steps: [1]:

1. *integral representation* for field functions approximations (also known as *kernel approximation*);
2. *particle approximation*: replaces the integral representation of the field functions and their derivatives by a sum over the values of the neighboring particles in the so-called support domain;
3. the particle approximations are performed to all terms related to field functions in the governing PDEs, producing a set of ordinary differential equations (ODEs) where the independent variable is the time;
4. the resulting ODEs are solved using either an explicit or an implicit integration algorithm.

3.1 Integral representation of a function

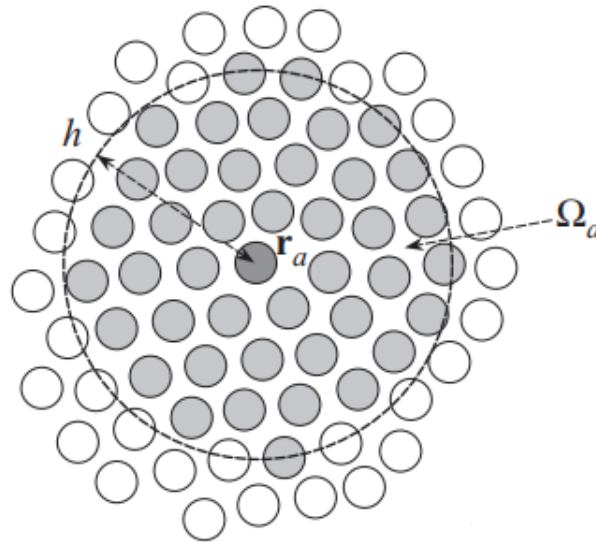
The integral interpolation theory is the base of SPH method fundamentals. In this formulation, within a domain Ω which contains a point x , we use convolution to obtain the integral representation of a function $f(x)$, such as [1]:

$$\langle f(x) \rangle = \int_{\Omega} f(x') W(x - x', h) dx' \quad (7)$$

where f is a function of the position x , $W(x - x', h)$ is the smoothing function with compact support (also called kernel function or smoothing kernel function). Besides, h is the smoothing length, which controls the influence area of W (it defines what are the neighboring particles of a given particle, as Fig. 1 depicts).

The kernel is fundamental for determining the approximation pattern, the size of the support domain, and the consistency and accuracy of the approximations [1]. Consequently, it must satisfy some criteria. Aside from the compact support condition, the normalization condition, smoothness, symmetry, and the Delta function property [1].

In the present work, the kernel used is the cubic spline proposed by Monaghan and Lattanzio [11],


 Figure 1: Domain Ω of a given particle a .

$$W(r, h) = \alpha_d \begin{cases} 1 - \frac{3}{2}q^2 + \frac{3}{4}q^3 & \text{if } 0 \leq q \leq 1 \\ \frac{1}{4}(2 - q)^3 & \text{if } 1 \leq q \leq 2 \\ 0 & \text{if } q \geq 2 \end{cases}$$

where $\alpha_d = \frac{10}{7\pi h^2}$ for two-dimensional problems, and $\frac{1}{\pi h^3}$ for three-dimensional problems.

The compact support allows us to replace the integral over the entire domain Ω by a summation over the influence area of the chosen particle (in the so-called smoothing length). Consequently, in the SPH method, the properties of a particle are evaluated by weighing the properties of neighboring particles. Thus, in the SPH formalism, the particle approximation of a function [1] is:

$$\langle f(x_i) \rangle = \sum_{j=1}^N \frac{m_j}{\rho_j} f(x_j) W_{ij}^h. \quad (8)$$

In this equation, $\langle f(x_i) \rangle$ is the approximation for function f at the position of fixed particle i ; $f(x_j)$ is the approximation for function f at the neighboring particle j ; m_j is the mass of particle j ; ρ_j represents the density of neighboring particle j ; W_{ij}^h is the kernel evaluated at position $x_i - x_j$ and N is the number of neighboring particles for particle i .

From Eq. (8), we can obtain the expressions for the gradient and divergent operators in the SPH formalism [1]:

$$\langle \nabla \otimes f(x_i) \rangle = \sum_{j=1}^N \frac{m_j}{\rho_j} \nabla_i W_{ij}^h \otimes f(x_j) \quad (9)$$

and

$$\langle \nabla \cdot f(x_i) \rangle = \sum_{j=1}^N \frac{m_j}{\rho_j} \nabla_i W_{ij}^h \cdot f(x_j). \quad (10)$$

Here, $W_{ij}^h = W(r_{ij}, h)$, and considering particle i , we evaluate the gradient such that:

$$\nabla_i W_{ij}^h = \frac{x_{ij}}{r_{ij}} \frac{\partial W_{ij}^h}{\partial r_{ij}} \quad (11)$$

where x_{ij} and r_{ij} represent the distance separating particles i and j ($x_{ij} = x_i - x_j$, and $r_{ij} = |x_i - x_j|$) [12].

3.2 Discretized balance equations

After introducing the basics of the method and the particle approximation, we proceed with the discretization stage of the governing equations. Considering $v_{ij} = v_i - v_j$, we can express the discretized form of the continuity equation (1) as [13]

$$\frac{D\rho_i}{Dt} = \sum_{j=1}^N m_j v_{ij} \cdot \nabla W_{ij}^h \quad (12)$$

and, for the Navier-Stokes equation (4),

$$\frac{D\mathbf{v}_i}{Dt} = - \sum_{j=1}^N m_j \left(\frac{P_i + P_j}{\rho_i \rho_j} + \Lambda_{ij} \right) \nabla_i W_{ij} - 2a\rho_a^2 \sum_{j=1}^N \frac{m_j}{\rho_j} \nabla_i W_{ij} + \mathbf{F}_s + \mathbf{g} \quad (13)$$

where Λ_{ij} is the term introducing the artificial viscosity [1] (the viscous dissipation term was not directly discretized) as follows:

$$\Lambda_{ij} = \begin{cases} \frac{-\alpha_\mu \bar{c}_{ij} \mu_{ij}}{\bar{\rho}_{ij}} & \text{if } v_{ij} \cdot r_{ij} < 0 \\ 0 & \text{if } v_{ij} \cdot r_{ij} > 0 \end{cases}$$

where c is the sound speed, and the average values for the sound speed and density are respectively $\bar{c}_{ij} = 0,5(c_i + c_j)$ and $\bar{\rho}_{ij} = 0,5(\rho_i + \rho_j)$. We must choose the value of α such as the energy transfer rate, due to the viscous dissipation, has its effects taking into account [1]. The introduction of an artificial viscosity aims to avoid the emergence of numerical instabilities and the interpenetration between particles, even for inviscid flows [9].

In addition, \mathbf{F}_s represents the external force added to take into account the effects of surface tension [14]

$$\mathbf{F}_s = \sum_j m_j \frac{\Pi_i^{\alpha\beta} + \Pi_j^{\alpha\beta}}{\rho_i \rho_j} \frac{\partial W}{\partial r_{ij}} \quad (14)$$

in which we evaluate the surface stress tensor using

$$\mathbf{\Pi}_i^{\alpha\beta} = \sigma^{\alpha\beta} \frac{1}{|\nabla C_i^{\alpha\beta}|} \left(\frac{1}{d} |\nabla C_i^{\alpha\beta}|^2 \mathbf{I} - \nabla C_i^{\alpha\beta} \otimes \nabla C_i^{\alpha\beta} \right) \quad (15)$$

where we introduced the gradient for the color function C , for phase α , given by

$$C_i^\alpha = \begin{cases} 1 & \text{if } i \in \alpha \\ 0 & \text{if } i \notin \alpha \end{cases} \quad (16)$$

which only exists in the presence of neighboring particles belonging to phase β ($\beta \neq \alpha$), such as [14]

$$\nabla C_i^{\alpha\beta} = \sum_j \frac{m_j}{\rho_j} (C_j^\beta - C_i^\beta) \frac{\partial W}{\partial r_{ij}}. \quad (17)$$

4 Aspects/Characteristics of the DualSPHysics software

Using C++ as the programming language, DualSPHysics is a numerical implementation of the SPH method developed to simulate realistic engineering problems using up to millions of particles and has a parallelized version based on OpenMP and CUDA APIs [15]. In the present work, we used multiphase version 4.0, available at <https://dual.sphysics.org>.

4.1 Particle repositioning

When we use the SPH method, we can sometimes face an instability called anisotropic particle spacing. It occurs due to the agglutination of particles [15]. DualSPHysics uses a modified version of the algorithm proposed by Xu et al. [16] to reposition particles (shifting algorithm). In this technique, particles are periodically moved to zones with lower particle concentrations to allow the domain to maintain a uniform distribution of particles, eliminating unwanted voids.

4.2 Temporal evolution and time step

In solving the system of ordinary equations, the temporal evolution algorithm chosen was the Verlet numerical integration scheme [17]. For an isothermal flow, we consider the shortened version of the governing equations:

$$\frac{D\mathbf{v}_a}{Dt} = \mathbf{F}_a, \quad (18)$$

$$\frac{D\rho_a}{Dt} = R_a, \quad (19)$$

$$\frac{D\mathbf{r}_a}{Dt} = \mathbf{v}_a, \quad (20)$$

$$\frac{D\mathbf{r}_a}{Dt} = \mathbf{v}_a, \quad (21)$$

$$\frac{D\mathbf{r}_a}{Dt} = \mathbf{v}_a, \quad (22)$$

where the first equation stands for the momentum equation, the following for the continuity equation, and we use the third equation to calculate the displacement of fluid particles.

For example, we usually employ the Verlet scheme in molecular dynamics due to its low computational cost. It is an explicit second-order method that does not require multiple steps at each time iteration. When we use the Verlet method to the resolution of quasi-compressible flow, as in the case of DualSPHysics, we calculate the variables according to the following scheme:

$$\mathbf{v}_a^{n+1} = \mathbf{v}_a^{n-1} + 2\Delta t \mathbf{F}_a^n, \quad (23)$$

$$\mathbf{v}_a^{n+1} = \mathbf{v}_a^{n-1} + 2\Delta t \mathbf{F}_a^n, \quad (24)$$

$$\mathbf{r}_a^{n+1} = \mathbf{r}_a^n + \Delta t \mathbf{v}_a^n + \frac{1}{2} \Delta t^2 \mathbf{F}_a^n, \quad (25)$$

$$\mathbf{r}_a^{n+1} = \mathbf{r}_a^n + \Delta t \mathbf{v}_a^n + \frac{1}{2} \Delta t^2 \mathbf{F}_a^n, \quad (26)$$

$$\rho_a^{n+1} = \rho_a^{n-1} + 2\Delta t R_a^n. \quad (27)$$

Due to the nature of the method, the density and velocity values at time $n + 1$ are not coupled, given that they do not use the values evaluated at n (using only those available at $n - 1$). This fact can lead to the divergence of the method [13]. Therefore, an intermediate step is required:

$$\mathbf{v}_a^{n+1} = \mathbf{v}_a^n + \Delta t \mathbf{F}_a^n, \quad (28)$$

$$\mathbf{v}_a^{n+1} = \mathbf{v}_a^n + \Delta t \mathbf{F}_a^n, \quad (29)$$

$$\mathbf{r}_a^{n+1} = \mathbf{r}_a^n + \Delta t \mathbf{v}_a^n + \frac{1}{2} \Delta t^2 \mathbf{F}_a^n, \quad (30)$$

$$\mathbf{r}_a^{n+1} = \mathbf{r}_a^n + \Delta t \mathbf{v}_a^n + \frac{1}{2} \Delta t^2 \mathbf{F}_a^n, \quad (31)$$

$$\rho_a^{n+1} = \rho_a^n + 2\Delta t R_a^n, \quad (32)$$

where the superscript n represents the current time and $t = n\Delta t$.

We must fulfill a Courant-Friedrichs-Lewy (CFL) condition to ensure that the Verlet method is stable, given that it is an explicit method [13]. So, we obtain the time step as follows

$$\Delta t = C_{CFL} \min(\Delta t_f, \Delta t_{cv}) \quad (33)$$

$$\Delta t_f = \min_a \left(\sqrt{\frac{h}{|f_a|}} \right), \quad (34)$$

$$\Delta t_{cv} = \min_a \left(\frac{h}{c_s + \max_b \left(\frac{h \mathbf{v}_a \cdot \mathbf{r}_a}{r_{ab}^2 + \eta^2} \right)} \right), \quad (35)$$

where C_{CFL} is a multiplicative factor, Δt_f is obtained from the evaluated force f_a per mass unit acting on particle a , and Δt_{cv} is the estimate for the ratio between the particle displacement (r_a) and its velocity (v_a), plus the speed of sound (c_s).

4.3 Boundary conditions

We represent the domain boundaries by a set of particles treated separately from the fluid particles. In DualSPHysics software, the standard boundary condition is called dynamic boundary condition. In this condition, we apply the same governing equations to the particles placed on the boundaries. However, they do not move due to the forces acting on them [15]. When a fluid particle approaches a boundary, and the distance between them becomes twice as small as the smoothing length h , the density of boundary particles has its value increased, causing a pressure increment. Consequently, a repulsive force is created and exerted on the approaching fluid particle due to the pressure contribution in the momentum equation.

5 Results

We start by checking the accuracy of the numerical code results. With this purpose in mind, we solve the modified Couette flow problem, which is a flow of two fluids with different viscosities and densities between two parallel plates.

After that, we addressed the two-phase flow in a horizontal pipe. We performed this using two reservoirs that store the two different fluids. Then, we inject the fluids into the pipeline through a Y-shaped connection.

5.1 Modified Couette flow

In the modified Couette flow, as described by Alvarado-Rodríguez et al. [7], the flux occurs between two infinite parallel plates for two fluids with distinct densities (ρ_1 and ρ_2) and viscosities (μ_1 and μ_2).

In this problem, there is a laminar flow between the plates. The upper plate is moving in the x -direction while we keep the lower plate at rest. The initial velocity for the plate at the top is $V = 1.0 \times 10^{-3}$ m/s in the x -axis positive direction, the distance separating each plate is $y = 0.001$ m, with each fluid phase filling half of the total height ($h_1 = h_2 = 0.0005$ m), as shown in Fig. 2.



Figure 2: Geometric configuration for the modified Couette flow.

Now, we simulate the infinite domain by introducing periodic boundary conditions, applied even for the particles that represent the horizontal plates. Table 1 holds the other parameters used in this simulation, such as physical properties for each fluid.

Table 1: Parameters used for the Couette flow.

Parameter	Symbol	Value
Distance between particles	dp	5.0×10^{-5} m
Density for Phase 1	ρ_1	1,000 kg/m ³
Density for Phase 2	ρ_2	2,000 kg/m ³
Viscosity for Phase 1	μ_1	0.5×10^{-6} m ² /s
Viscosity for Phase 2	μ_2	1.0×10^{-6} m ² /s

For this specific problem, we know that there is an analytical solution [13]. It provides the theoretical velocities, for each phase (v_{ρ_1} and v_{ρ_2}), in a steady-state regime as a function of the height y :

$$v_{\rho_1} = \left(\frac{V}{\mu_2 h_1 + \mu_1 h_2} \right) [\mu_1 (y - h_1) + \mu_2 h_1], \quad (36)$$

$$v_{\rho_2} = \left(\frac{\mu_2 V}{\mu_2 h_1 + \mu_1 h_2} \right) y. \quad (37)$$

Figure 3 shows the comparison between the theoretical velocities and those obtained numerically, acquired in 21 equally spaced points along the y -axis, at the middle point of the total length in the x -axis.

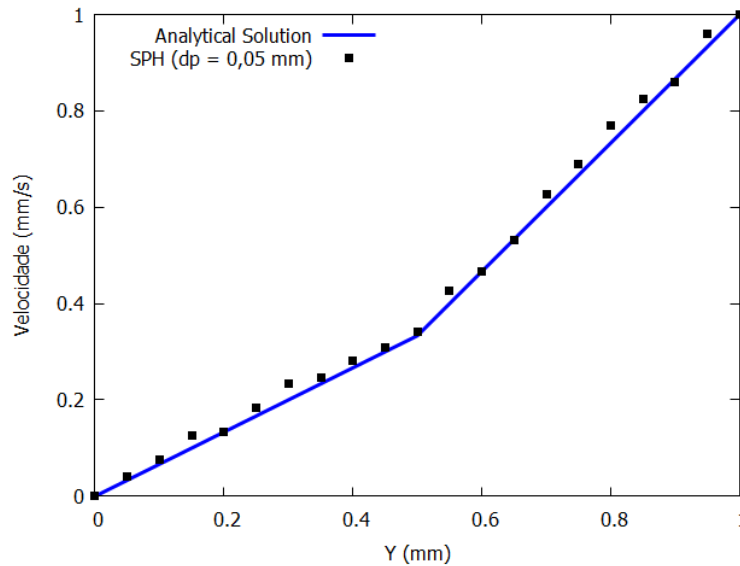


Figure 3: Velocity profiles for the Couette flow problem.

As we can see in the figure, the numerical values are very close to the theoretical. We found even that some numerical values overlapping parts of the theoretical curve. Additionally, the velocity for particles in contact with the lower plate is zero, as Eq. (36) predicts, and has its maximum value for particles near the plate upper plate, in agreement with Eq. (37). We also observe the correct representation for the change in the profile around $y=0.0005$ m, which defines the position of the fluid separation interface.

From the values obtained through the analytical solution, we can estimate the accuracy of the numerical results by evaluating the relative mean square error,

$$\%RMSE = 100 \times \sqrt{\frac{1}{N} \sum (v_{SPH} - v_{exact})^2} \quad (38)$$

where N is the number of data points, v_{SPH} is the velocity obtained with the SPH method, and v_{exact} is the analytical velocity value. In the present case, we obtained a value of $1.94 \times 10^{-5}\%$ for the relative error. Therefore, we can conclude that the numerical results accurately reproduced the values predicted by the theory.

5.2 Two-phase flow in a horizontal pipe

In this flow, we seek to identify the flow regimes reported by Alvarado-Rodríguez et al. [7]. We display in Fig. 4 the geometry (not at scale) that represents the problem domain.

The main pipe section, where the two-phase flow occurs, is 3.00 m long with a diameter of 20 mm. We use a Y-shaped connection with $\theta = 45^\circ$ to inject the fluids and cause them to mix. Each injection section has the same diameter $d_1=d_2=10$ mm, with the upper phase corresponding to oil and the lower representing the water. The two input sections act as reservoirs, maintaining the flow in the main section of the pipe, where it is analyzed.

In all simulations, we utilized 7.5×10^{-5} m as the initial distance between particles and 840 kg/m^3 and 998 kg/m^3 for the densities of Phases 1 and 2, respectively. We considered four sets of velocities, as presented in Table 2.

Figure 5 shows the flow patterns obtained for each of the four sets of velocities from Table 2. We acquired the results in the pipe section directly after the phases insertion zone. Then, we created the visualization patterns that we observe in this figure using the densities values of each phase.

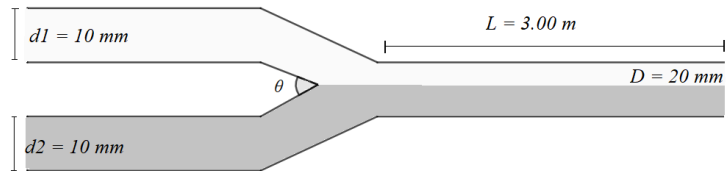


Figure 4: Geometric configuration for the horizontal pipe problem.

Table 2: Initial velocities for each phase.

Test case	Velocity of Phase 1	Velocity of Phase 2
1	0.085 m/s	0.16 m/s
2	0.250 m/s	0.20 m/s
3	0.085 m/s	1.00 m/s
4	0.650 m/s	0.16 m/s

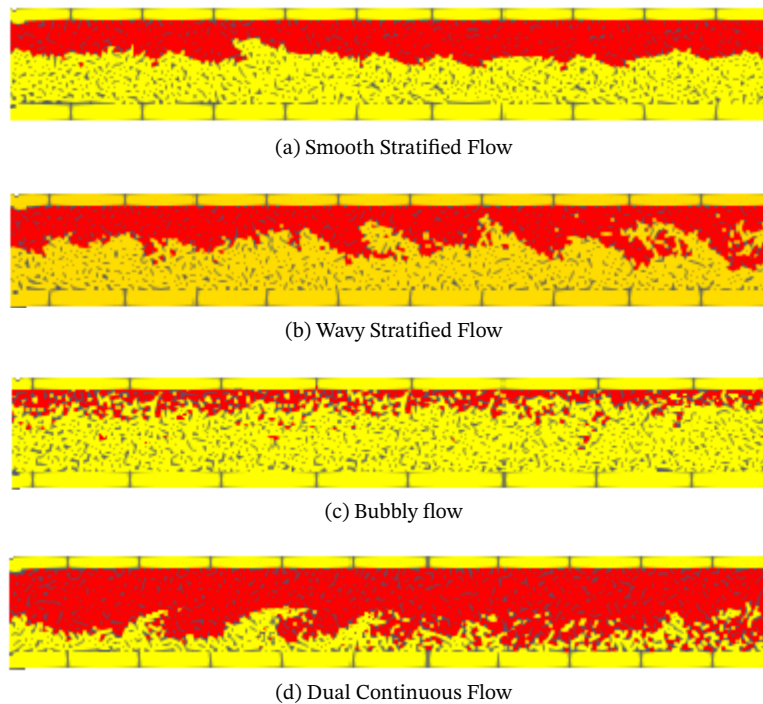


Figure 5: Visualization of the flow patterns for Cases 1, 2, 3 and 4. Color map depicts the density.

Case 1, Fig. 5a, represents the regime known as *Smooth Stratified Flow*, which occurs when the relative velocities for the phases are low, and there is a complete gravitational separation. We can observe a clear separation between the fluids with a smooth interface. We think that we correctly identified this regime.

The second regime (Fig. 5b), Case 2, corresponds to the *Wavy Stratified Flow* regime, on which, even though the phases are separated, there is a higher undulation in the fluid separation interface. This flow pattern appears when the velocity of the fluid with lower density is increased compared to that used in the smooth stratified flow.

For the following result, Case 3 and Fig. 5c, the identified regime is classified as *Bubbly flow*, occurring when we increase the velocity of the heavier phase. In this case, we maintain the velocity of the lighter phase equal to that of the smoothed stratified flow. For this flow pattern, we note the dispersion of the phase oil in the phase water as discrete bubbles. The continuity of the lighter phase is limited to the upper section of the pipe.

Lastly, we highlight that Case 4 matches the *Dual Continuous Flow* regime. With the increase in velocity for the lighter phase, the stratified regime transforms into this new pattern. Its characteristic is the maintenance of some phase continuity in the upper and lower pipe areas. Nevertheless, there is now a dispersion of both fluids. As we can verify, Fig. 5d corresponds to the related behavior, confirming that we rightly captured the reference regime with the simulation using DualSPHysics.

6 Conclusions

We studied the feasibility of using the DualSPHysics numerical code, based on the SPH method, to simulate two-phase oil-water flows in pipes.

For the modified Couette flow problem, the obtained numerical solution showed good agreement with the analytical solution. The analysis of the relative error indicated the accuracy of the results obtained with the DualSPHysics.

Finally, in the test cases for the two-phase oil-water flow, both fluids are injected into the main horizontal pipe using a Y-shaped connection. It was possible to identify some of the typical flow patterns in horizontal tubes, matching those expected for the initial velocity ranges imposed to each phase. In this way, we understood that the appropriate capture of the flow regimes demonstrates the potential and feasibility of using DualSPHysics to simulate two-phase flows in horizontal pipes.

Acknowledgments

This study was financed in part by the Coordination of Superior Level Staff Improvement - Brasil (CAPES) - Finance Code 001.

References

- [1] G. Liu and M. Liu, *Smoothed Particle Hydrodynamics: A Meshfree Particle Method*. Singapore: World Scientific, 2003.
- [2] L. Lucy, "A numerical approach to the testing of the fission hypothesis," *The Astronomical Journal*, vol. 82, pp. 1013–1024, 1977. Available at: <https://ui.adsabs.harvard.edu/abs/1977AJ.....82.1013L>
- [3] R. Gingold and J. Monaghan, "Smoothed particle hydrodynamics: theory and application to non-spherical stars," *Monthly Notices of the Royal Astronomical Society*, vol. 181, pp. 375–389, 1977. Available at: <https://doi.org/10.1093/mnras/181.3.375>
- [4] O. Shoham and S. of Petroleum Engineers of AIME., *Mechanistic Modeling of Gas-liquid Two-phase Flow in Pipes*. Society of Petroleum Engineers, 2006.
- [5] A. Hasan and C. Kabir, *Fluid Flow and Heat Transfer in Wellbores*. United States: Society of Petroleum Engineers, 2016.
- [6] T. Douillet-Grellier, F. De Vuyst, H. Calandra, and P. Ricoux, "Simulations of intermittent two-phase flows in pipes using smoothed particle hydrodynamics," *Computers & Fluids*, vol. 177, pp. 101–122, 2018. Available at: <https://doi.org/10.1016/j.compfluid.2018.10.004>
- [7] C. Alvarado-Rodríguez, J. Klapp, J. Domínguez, A. Uribe-Ramírez, J. Ramírez-Minguela, and M. Gómez-Gesteira, *Multiphase Flows Simulation with the Smoothed Particle Hydrodynamics Method*. Springer International Publishing, 2019. Available at: <http://dx.doi.org/10.1007/978-3-030-38043-4>
- [8] J. Slattery and A. Varma, *Advanced Transport Phenomena*, ser. Cambridge Series in Chemical Engineering. Cambridge University Press, 1999.
- [9] C. A. D. Fraga Filho, *Smoothed Particle Hydrodynamics: Fundamentals and Basic Applications in Continuum Mechanics*. Springer, 2019.
- [10] A. Mokos, "Multi-phase modelling of violent hydrodynamics using smoothed particle hydrodynamics (sph) on graphics processing units (gpu)," Ph.D. dissertation, School of Mechanical, University of Manchester, Manchester, United Kingdom, 2014. Available at: <https://ethos.bl.uk/OrderDetails.do?uin=uk.bl.ethos.617969>

- [11] J. Monaghan and J. Lattanzio, "A refined particle method for astrophysical problems," *Journal of Astronomy and Astrophysics*, vol. 149, pp. 135–143, 1985. Available at: <https://ui.adsabs.harvard.edu/abs/1985A&A...149.135M>
- [12] M. L. Góes, "Estudo de interfaces livres empregando o método Smoothed Particle Hydrodynamics (SPH) e as equações de estado de van der Waals e de Martin," Ph.D. dissertation, Polytechnic Institute, Rio de Janeiro State University, Nova Friburgo, Brazil, 2016. Available at: <http://www.bdt.d.uerj.br/handle/1/13703>
- [13] N. J. dos Santos Carvalho, "Simulação numérica do escoamento bifásico em um duto horizontal empregando o método smoothed particle hydrodynamics," Master's thesis, Polytechnic Institute, Rio de Janeiro State University, Nova Friburgo, Brazil, 2021. Available at: <http://www.bdt.d.uerj.br/handle/1/16413>
- [14] B. Lafaurie, C. Nardone, R. Scardovelli, S. Zaleski, and G. Zanetti, "Modelling merging and fragmentation in multiphase flows with SURFER," *Journal of Computational Physics*, vol. 113, no. 1, pp. 134–147, 1994. Available at: <https://doi.org/10.1006/jcph.1994.1123>
- [15] A. Crespo, J. Domínguez, B. Rogers, M. Gómez-Gesteira, S. Longshaw, R. Canelas, R. Vacondio, A. Barreiro, and O. García-Feal, "DualSPHysics: Open-source parallel CFD solver based on Smoothed Particle Hydrodynamics (SPH)," *Computer Physics Communications*, vol. 187, pp. 204–216, 2015. Available at: <https://doi.org/10.1016/j.cpc.2014.10.004>
- [16] R. Xu, P. Stansby, and D. Laurence, "Accuracy and stability in incompressible SPH (ISPH) based on the projection method and a new approach," *Journal of Computational Physics*, vol. 228, no. 18, pp. 6703–6725, 2009. Available at: <https://doi.org/10.1016/j.jcp.2009.05.032>
- [17] L. Verlet, "Computer "Experiments" on Classical Fluids - Thermodynamical Properties of Lennard-Jones Molecules," *Physical Review*, vol. 159, pp. 98–103, 1967. Available at: <https://link.aps.org/doi/10.1103/PhysRev.159.98>